Effect of Friction Stir Processing on the Kinetics of Superplastic Deformation in an Al-Mg-Zr Alloy

Z.Y. MA, R.S. MISHRA, M.W. MAHONEY, and R. GRIMES

The effect of friction stir processing on the superplastic behavior of extruded Al-4Mg-1Zr was examined at 350 °C to 600 °C and at initial strain rates of 1×10^{-3} to 1 s^{-1}. A combination of a fine grain size of 1.5 μm and high-angle grain boundaries in the friction stir–processed (FSP) alloy led to considerably enhanced superplastic ductility, much-reduced flow stress, and a shift to a higher optimum strain rate and lower optimum temperature. The as-extruded alloy exhibited the highest superplastic ductility of 1015 pct at 580 °C and an initial strain rate of $1 \times 10^{-2}s^{-1}$, whereas a maximum elongation of 1280 pct was obtained at 525 °C and an initial strain rate of $1 \times 10^{-1}s^{-1}$ for the FSP alloy. The FSP alloy exhibited enhanced superplastic deformation kinetics compared to that predicted by the constitutive relationship for superplasticity in fine-grained aluminum alloys. A possible origin for enhanced superplastic deformation kinetics in the FSP condition is proposed.

I. INTRODUCTION

A prerequisite for achieving structural superplasticity is a fine grain size, typically less than 15 μm. Various processing techniques such as thermomechanical processing (TMP),[1,2] equal-channel angular pressing,[3] torsional deformation under pressure,[4] and friction stir processing[5,6] have been developed to produce fine-grained aluminum alloys. Among these, friction stir processing, developed based on the principles of friction stir welding (FSW),[7–11] is particularly attractive because it provides a very simple and effective approach for obtaining fine-grained regions for specialized applications. Grain sizes ranging from 0.8 to 12 μm have been reported by various investigators in the friction stir–welded and FSP aluminum alloys.[5,6,8–11] More importantly, friction stir processing can result in the generation of high-strain-rate superplasticity (HSRS) in commercial aluminum alloys. A recent study[12] has indicated that FSP 7075Al with a fine grain size of 3.8 μm exhibited HSRS. A superplastic ductility of >1250 pct was obtained at 480 °C and high strain rates of 3×10^{-3} to $3 \times 10^{-2}s^{-1}$. The optimum strain rate for the FSP 7075Al was more than one order of magnitude higher than the previous best TMP effort on 7075Al.[2] This shows that friction stir processing is a very effective processing approach to produce fine-grained materials amenable to HSRS. Furthermore, the FSP aluminum alloy exhibited a much lower cavity level and higher critical strain for cavitation compared to the TMP alloy.[13]

However, fine grain size is a necessary, but not always sufficient, condition to obtain superplasticity. If the fine-grained microstructure is not stable at high temperature, superplastic elongation will be significantly reduced. A recent study[14] revealed that fine-grained 7475Al prepared by friction stir processing did not exhibit superplastic elongation due to abnormal grain growth at high temperatures. Similarly, abnormal grain growth was also observed at high temperatures in the FSP 7050 and 2519 aluminum alloys.[15] Fine Al_3Zr dispersoids can inhibit grain growth in fine-grained aluminum alloys at high temperature. Supral aluminum alloys (Al-Cu-Zr) have exhibited good superplasticity at a high strain rate of $10^{-2}s^{-1}$.[16,17] Recently, Grimes and coworkers[18,19] developed an Al-Mg-Zr alloy for enhanced superplastic properties. They showed that very good superplasticity was obtained in this alloy by a simple two-step process (extrusion plus cold rolling). As-cold-rolled Al-Mg-Zr exhibited elongations of >500 pct at a high strain rate of $1 \times 10^{-2}s^{-1}$.

In an initial study,[20] we reported that FSP Al-4Mg-Zr exhibited significantly enhanced superplasticity at a high strain rate of $1 \times 10^{-1}s^{-1}$. Furthermore, the strain-rate sensitivity of FSP Al-4Mg-1Zr increased with increasing strain rate from 1×10^{-3} to 1 s^{-1} at temperatures of 450 °C and 525 °C. This behavior is different from that of FSP 7075Al, in which the strain-rate sensitivity was constant within the temperature range of 470 °C to 500 °C and the strain-rate range of 1×10^{-3} to 1×10^{-1} s^{-1}. The trend observed in FSP Al-4Mg-1Zr indicates that either a threshold stress is operative, or the deformation mechanism changes. In this work, additional tensile tests were conducted at 425 °C and 500 °C for the strain-rate range of 1×10^{-3} to 1 s^{-1} for FSP Al-4Mg-1Zr, and the superplastic mechanism was evaluated. For comparison, the superplastic behavior of as-extruded Al-4Mg-1Zr was also examined in the temperature range of 350 °C to 600 °C and the initial strain-rate range of 1×10^{-3} to 1 s^{-1}. The purpose of this study was fourfold: (1) to establish the optimum superplasticity deformation temperature and strain rate of as-extruded Al-4Mg-1Zr, (2) to investigate the effect of friction stir processing on the superplastic behavior, (3) to identify the operative superplastic deformation mechanism in both the as-extruded and FSP conditions, and (4) to compare the deformation kinetics of both as-extruded and FSP Al-4Mg-1Zr with that predicted by the constitutive relationship for superplasticity in fine-grained aluminum alloys.

Z.Y. MA, Professor, formerly with the Department of Materials Science and Engineering, University of Missouri, is with the Institute of Metal Research, Chinese Academy of Sciences, Shenyang 110016, P.R. China. R.S. MISHRA, Associate Professor, is with the Department of Materials Science and Engineering, University of Missouri, Rolla, MO 65409. Contact e-mail: rsmishra@umr.edu M.W. MAHONEY is with Rockwell Scientific, Thousand Oaks, CA 91360. R. GRIMES is with the Department of Materials, Imperial College of Science, Technology and Medicine, London, SW7 2BP, United Kingdom.

Manuscript submitted January 19, 2004.

II. EXPERIMENTAL

Al-4Mg-1Zr was obtained as a 10 × 20 mm extruded bar. Fabrication of the extrusion has been described in detail in previous works.[18,19] A single-pass FSP with a processing parameter of 4 inches per minute (ipm) /350 rpm was made using conventional FSW practices, where ipm denotes the traverse speed of the tool and rpm denotes the rotation rate of the tool. The microstructures of both the as-extruded and FSP materials were examined by a PHILIPS* EM430 transmission electron microscope (TEM). The TEM specimens were prepared by the ion-milling technique. Differential thermal analysis (DTA) was conducted on the as-extruded alloy with a heating speed of 10 K/min.

*PHILIPS is a trademark of Philips Electronic Instruments Corp., Mahwah, NJ.

To evaluate the superplastic behavior of the FSP region, mini tensile specimens with a 1.3 mm gage length were electrodischarge machined from the FSP region in the transverse direction, ground, and polished to a final thickness of 0.5 mm. Constant-crosshead-speed tensile tests were conducted using a computer-controlled, custom-built mini tensile tester. For comparison, tensile tests were also conducted under the same conditions on the as-extruded material, with the tensile axis parallel to the extrusion direction. The surfaces of deformed specimens were examined on a JEOL* T330A scanning electron microscope (SEM). Extruded Al-4Mg-1Zr specimens deformed at 550 °C and an initial strain rate of 1×10^{-2} s^{-1} to a strain of 1.0 and 1.3, respectively, were interrupted and subjected to TEM examination.

*JEOL is a trademark of Japan Electron Optics Ltd., Tokyo.

III. RESULTS

A. *Microstructural Characteristics*

Figures 1(a) and (b) show the microstructure of the as-extruded Al-4Mg-1Zr. Two observations can be made. First, the microstructure was characterized by predominantly low-angle grain boundaries, with grains/subgrains aligned along the extrusion direction. Second, the grain size was nonuniform.

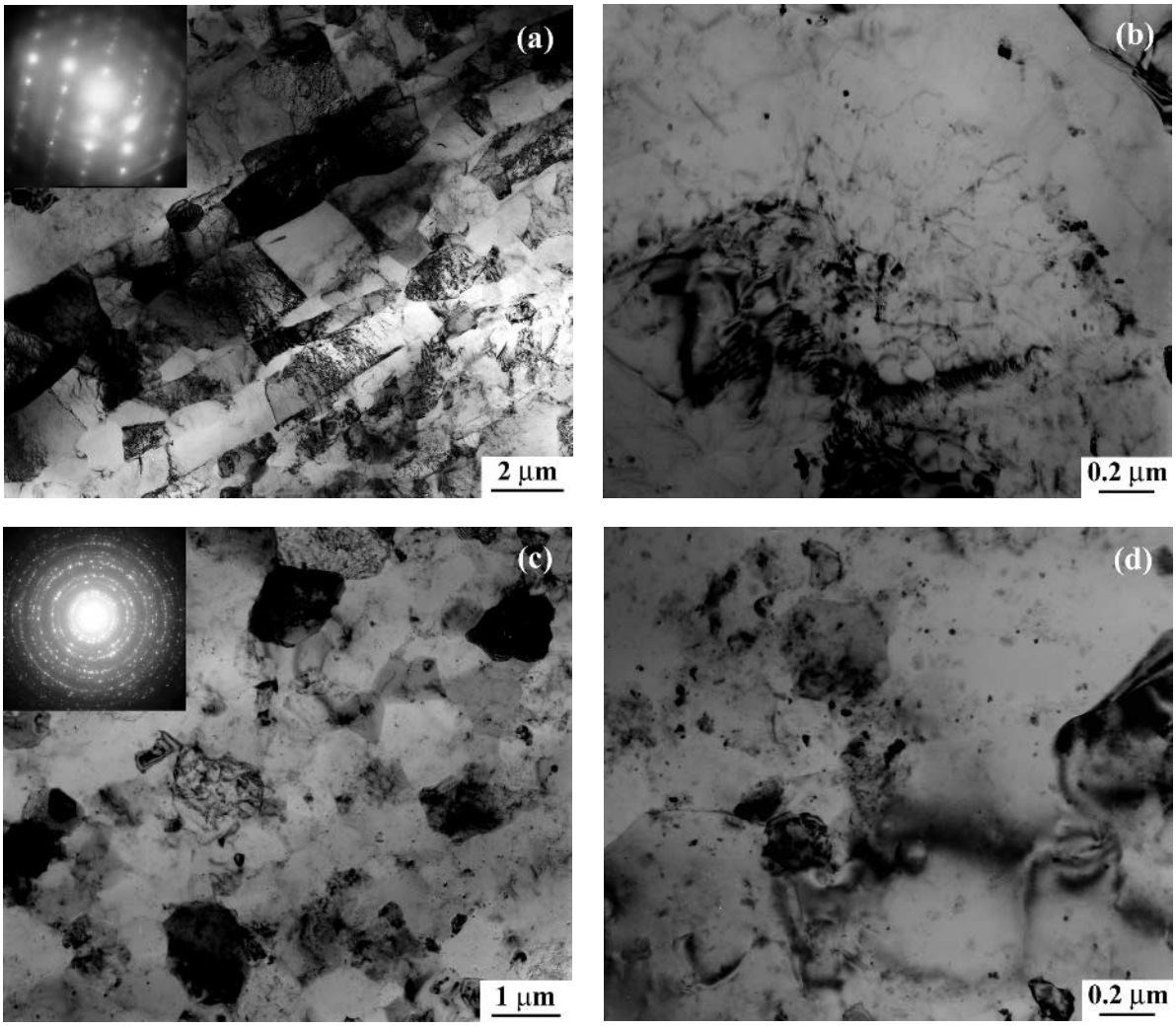

Fig. 1—TEM micrographs showing (*a*) grains in as-extruded Al-4Mg-1Zr, and (*b*) Al_3Zr particles in as-extruded Al-4Mg-1Zr, (*c*) grains in FSP Al-4Mg-1Zr and (*d*) Al_3Zr particles in FSP Al-4Mg-1Zr.

The average subgrain sizes in the directions parallel (d_L) and normal (d_T) to the extrusion direction were determined by the mean linear-intercept technique (subgrain size = 1.78 × the mean linear intercept) to be 1.9 and 1.7 μm (averaging above 250 grains), respectively. Thus, the average subgrain size (d) was determined to be 1.8 μm ($d = (d_L d_T)^{1/2}$). The dispersoids in the alloy were determined to be Al_3Zr by energy-dispersive spectrometry. The average size of Al_3Zr dispersoids was estimated to be 21.7 ± 11.8 nm (averaging 140 dispersoids).

Figures 1(c) and (d) show the microstructure of the FSP zone in the FSP Al-4Mg-1Zr. The bright-field TEM image shows well-defined grain boundaries (Figure 1c). Generally, the FSP microstructure was characterized by uniform and equiaxed recrystallized grains with predominant high-angle boundaries. The average grain size, determined by the mean linear-intercept technique, was 1.5 μm (averaging 123 grains). Compared to the as-extruded alloy (Figure 1d), the FSP Al-4Mg-1Zr exhibited a more uniform distribution of Al_3Zr dispersoids (Figure 1d). The average size of Al_3Zr dispersoids in the FSP alloy was determined to be 19.5 ± 11.9 nm (averaging 140 dispersoids), which is similar to the as-extruded alloy.

B. *Superplastic Behavior*

1. *As-extruded alloy*

The stress-strain behavior of as-extruded Al-4Mg-1Zr is shown in Figure 2 as a function of initial strain rate and temperature. The optimum strain rate for maximum elongation at 580 °C was $1 \times 10^{-2} s^{-1}$. This shows that HSRS can be achieved in as-extruded Al-4Mg-1Zr. At an initial strain rate of 1×10^{-2} s^{-1}, the optimum temperature for maximum elongation was 580 °C. The stress-strain curves of as-extruded Al-4Mg-1Zr at 580 °C, for initial strain rates of 1×10^{-3} to 3×10^{-2} s^{-1}, were characterized by an initial strain hardening, intermediate strain softening, and then final (secondary) strain hardening (Figure 2(a)). Similar features were also observed at 1×10^{-2} s^{-1} for temperatures of 565 °C to 600 °C (Figure 2(b)). However, no secondary strain hardening was observed in as-extruded Al-4Mg-1Zr deformed at higher initial strain rates of $>3 \times 10^{-2}$ s^{-1} or lower temperatures of <565 °C.

Figure 3(a) shows the variation of superplastic ductility of as-extruded Al-4Mg-1Zr with initial strain rate at different temperatures. Optimum superplasticity was observed at a high strain rate of 1×10^{-2} s^{-1} for the temperature range of 450 °C to 580 °C. A maximum elongation of 1015 pct was obtained at 580 °C and an initial strain rate of 1×10^{-2} s^{-1}. Even at an initial strain rate of 1 s^{-1}, the as-extruded Al-4Mg-1Zr exhibited elongations of ~200 pct. Figure 3(b) shows the effect of test temperature on the superplastic elongation of as-extruded Al-4Mg-1Zr at different initial strain rates. For the initial strain rates of 1×10^{-1} and 1 s^{-1}, the superplastic elongation was independent of the temperature in the temperature

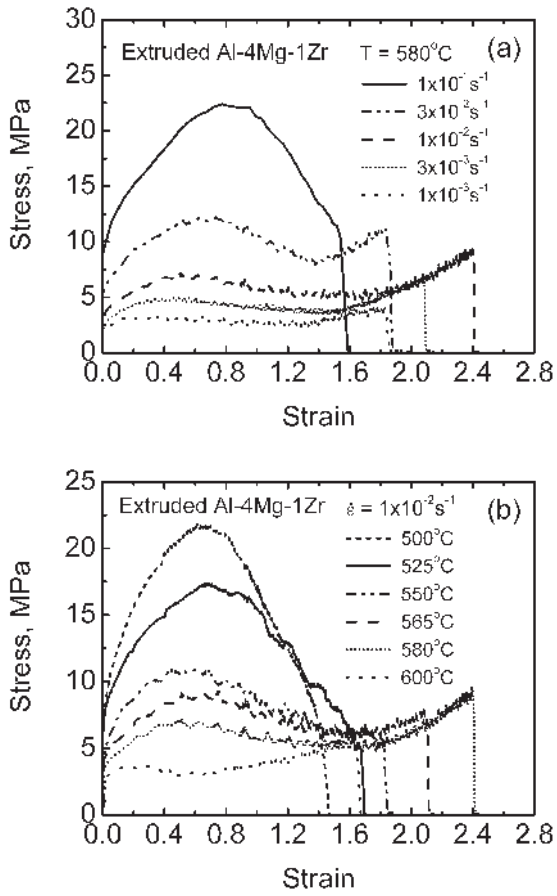

Fig. 2—Stress-strain behavior of as-extruded Al-4Mg-1Zr as a function of (*a*) initial strain rate at 580 °C and (*b*) temperature at an initial strain rate of 1×10^{-2} s^{-1}.

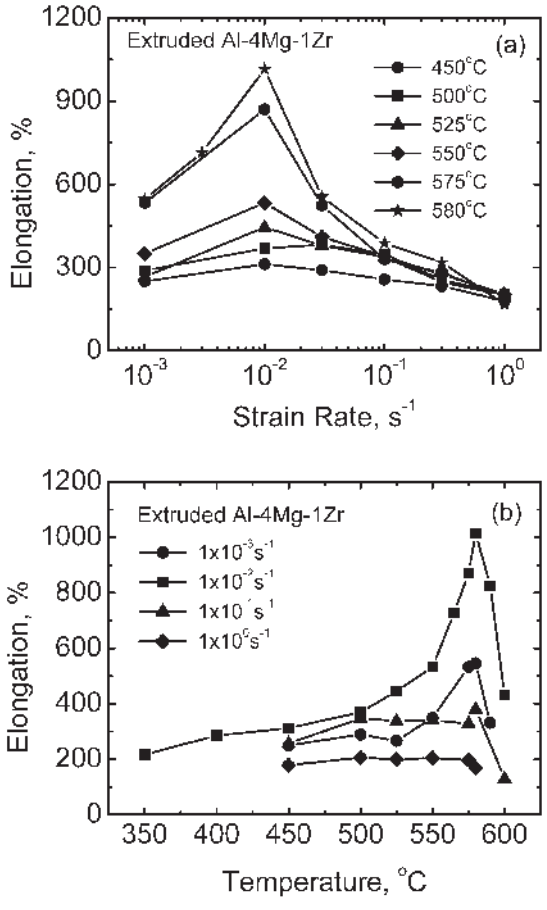

Fig. 3—Variation of elongation with (*a*) initial strain rate at different temperatures, and (*b*) temperature at different initial strain rates for as-extruded Al-4Mg-1Zr.

range of 500 °C to 580 °C. However, at the initial strain rates of 1×10^{-3} and 1×10^{-2} s^{-1}, the superplastic ductility of as-extruded Al-4Mg-1Zr increased with increasing temperature, and maximum ductility was observed at 580 °C. Above 580 °C, the superplasticity decreased rapidly for all strain rates. Even at a low temperature of 350 °C, as-extruded Al-4Mg-1Zr exhibited an elongation of 220 pct for the initial strain rate of 1×10^{-2} s^{-1}. This indicates that HSRS can be obtained in as-extruded Al-4Mg-1Zr over the wide temperature range of 350 °C to 600 °C.

Figure 4 shows the variation of flow stress (at a true strain of 0.1) with the initial strain rate for as-extruded Al-4Mg-1Zr. The strain-rate sensitivity (m) increased continuously with increasing initial strain rate from 1×10^{-3} to 1 s^{-1} at all investigated temperatures. For example, at 500 °C, as-extruded Al-4Mg-1Zr exhibited m values of ~0.24, 0.34, and 0.38 in the initial strain-rate ranges of 1×10^{-3} to 1×10^{-2} s^{-1}, 1×10^{-2} to 1×10^{-1} s^{-1}, and 1×10^{-1} to 1 s^{-1}, respectively.

2. *The FSP alloy*

The stress-strain behavior of FSP Al-4Mg-1Zr has been reported in a previous article.[20] Generally, the flow curves at 525 °C for the initial strain-rate range of 1×10^{-3} to 1 s^{-1} and at 1×10^{-1} s^{-1} for the temperature range of 350 °C to 550 °C showed extensive strain hardening. The level of strain beyond the peak stress was limited. Figure 5(a) shows the variation of superplastic elongation of FSP Al-4Mg-1Zr with initial strain rate at different temperatures. Optimum superplasticity was observed at a high strain rate of 1×10^{-1} s^{-1} (even 3×10^{-1} s^{-1} for 450 °C) at temperatures ranging from 425 °C to 525 °C. The maximum superplasticity of 1280 pct was obtained at 525 °C and 1×10^{-1} s^{-1}. This shows that the optimum superplasticity was achieved in FSP Al-4Mg-1Zr at a strain rate one order of magnitude higher than the extruded alloy and at a temperature lower by 55 °C. Figure 5(b) shows the effect of test temperature on the superplastic elongation of FSP Al-4Mg-1Zr at different initial strain rates. The FSP Al-4Mg-1Zr exhibited HSRS at 1×10^{-1} s^{-1} within the temperature range of 350 °C to 550 °C. Even at the low temperature of 350 °C, the FSP Al-4Mg-1Zr exhibited a high elongation of 330 pct. Furthermore, at the high temperature of 550 °C, a high elongation of 1210 pct indicates that the fine-grained microstructure in FSP Al-4Mg-1Zr is stable at high temperature. Even at a high strain rate of 1 s^{-1}, the FSP Al-4Mg-1Zr still exhibited elongations >450 pct in the temperature range of 450 °C to 525 °C.

Figure 6 shows the flow stress (at a true strain of 0.1)–initial strain-rate curves at different temperatures for FSP

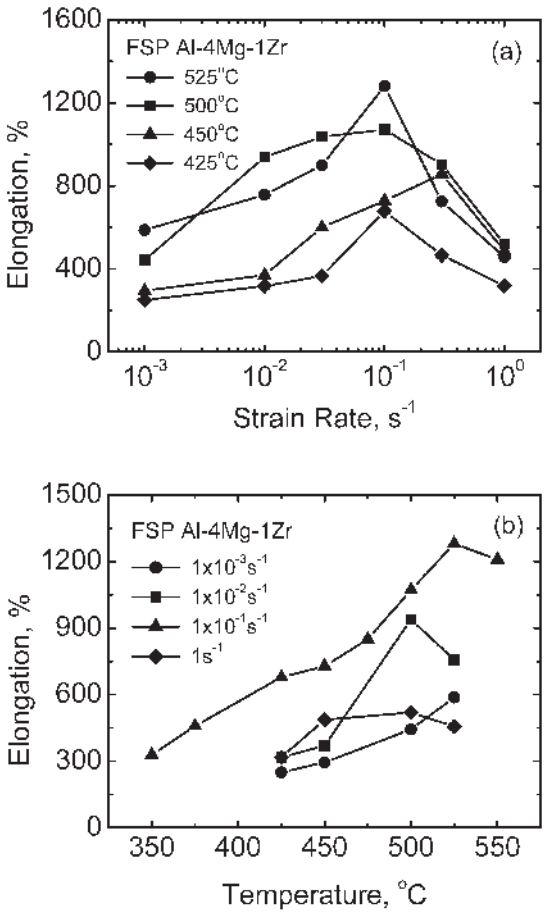

Fig. 5—Variation of elongation with (*a*) initial strain rate at different temperatures and (*b*) temperature at different initial strain rates for FSP Al-4Mg-1Zr.

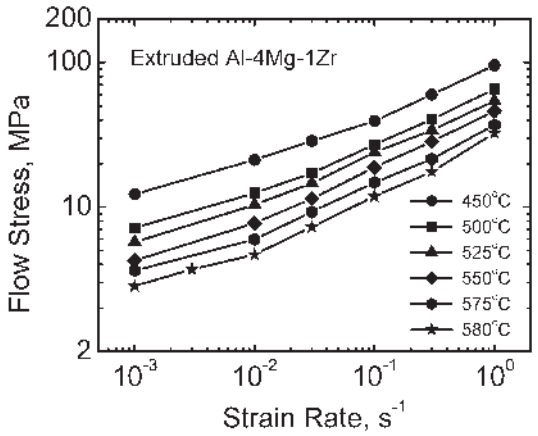

Fig. 4—Variation of flow stress with initial strain rate at different temperatures for as-extruded Al-4Mg-1Zr at a true strain of 0.1.

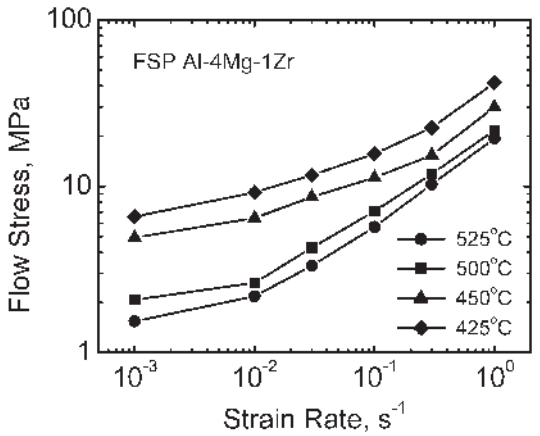

Fig. 6—Variation of flow stress with initial strain rate at different temperatures for FSP Al-4Mg-1Zr at a true strain of 0.1.

Al-4Mg-1Zr. Similar to as-extruded Al-4Mg-1Zr, FSP Al-4Mg-1Zr exhibited increasing strain-rate sensitivity with increasing initial strain rate from 1×10^{-3} to $1\ s^{-1}$ at the investigated temperatures. For example, at 525 °C, FSP Al-4Mg-1Zr exhibited an m value of ~0.15, 0.42, and 0.53 in the initial strain-rate ranges of 1×10^{-3} to $1 \times 10^{-2}\ s^{-1}$, 1×10^{-2} to $1 \times 10^{-1}\ s^{-1}$, and 1×10^{-1} to $1\ s^{-1}$, respectively.

C. *Microstructural Evolution during Superplastic Deformation*

Figure 7 shows surface morphologies of as-extruded Al-4Mg-1Zr deformed to various strains or failure at 550 °C and at an initial strain rate of $1 \times 10^{-2}\ s^{-1}$. At a strain of 0.6, evidence for grain-boundary sliding (GBS) of individual grains was observed in some regions (as marked by the letter A in Figure 7(a)). This is evidenced by a surface-relief pattern, *i.e.,* lifting or heaving of grain boundaries.[21,22,23] However, in most regions (as marked by the letter B in Figure 7(a)), sliding occurred by grain groups, known as cooperative grain-boundary sliding (CGBS), which is evidenced by lifting or heaving of a region containing several grains.[24,25] At a strain of 1.0, while the topography of the deformed specimen showed that most grains took part in GBS (Figure 7(b)), elongated groups of grains (marked by the letter C in Figure 7(b)) detected on the surface indicate that not all grains were involved in GBS as individual grains. At a strain of 1.3, nearly all grains took part in GBS, and most grains developed into striplike morphologies (Figure 7(c)). When the specimen was strained to failure, all the surface grains evolved into striplike morphologies, and individual grains are not readily discernable (Figure 7(d)). Furthermore, the SEM examinations revealed that at higher strain rates or lower temperatures, only some grains took part in GBS, and most grains in elongated grain groups did not individually slide (not shown). With decreasing strain rate or increasing temperature, more grains participated in GBS and the fraction involved in CGBS decreased (not shown).

For FSP Al-4Mg-1Zr, the grain aspect ratio did not change even after large deformation, indicative of the occurrence of GBS. The GBS of individual grains was observed to be dominant, and no CGBS was observed at the investigated strain-rate and temperature ranges (Figure 8(b)). Figure 8 shows the distinct difference between surface morphologies of as-extruded and FSP Al-4Mg-1Zr deformed to failure at 525 °C and a strain rate of $1 \times 10^{-1}\ s^{-1}$. The surface grain size in both the extruded and FSP Al-4Mg-1Zr increased with decreasing strain rate and increasing temperature. For example, in FSP Al-4Mg-1Zr deformed at 525 °C and a strain rate of $1 \times 10^{-1}\ s^{-1}$, surface grains grew to ~5 μm in size (Figure 8(b)).

Figure 9 shows TEM micrographs of as-extruded Al-4Mg-1Zr deformed at 550 °C and an initial strain rate of $1 \times 10^{-2}\ s^{-1}$ to various strains. At a strain of 1.0, a certain amount of nearly equiaxed grains, separated primarily

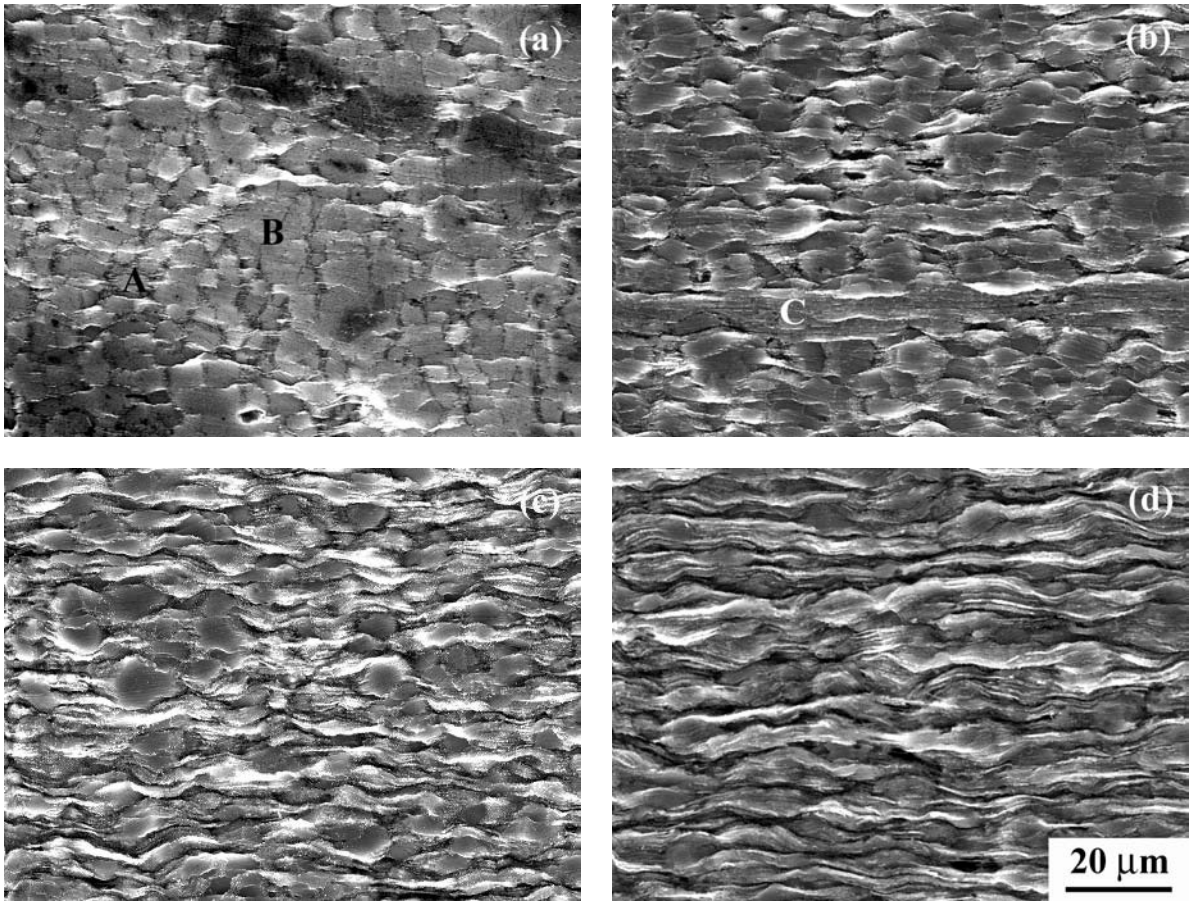

Fig. 7—SEM micrographs showing surface morphologies of as-extruded Al-4Mg-1Zr superplastically deformed at 550 °C and an initial strain rate of $1 \times 10^{-2}\ s^{-1}$ to a strain of (*a*) 0.6, (*b*) 1.0, (*c*) 1.3, and (*d*) to failure (tensile axis is horizontal).

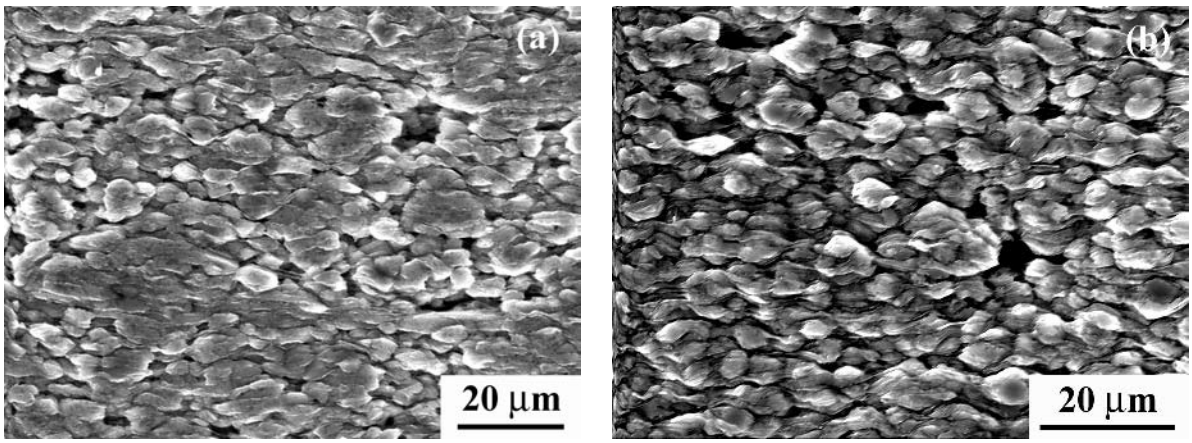

Fig. 8—SEM micrographs showing surface morphologies of Al-4Mg-1Zr superplastically deformed to failure at 525 °C and an initial strain rate of 1×10^{-1} s^{-1}: (*a*) as-extruded and (*b*) FSP (tensile axis is horizontal).

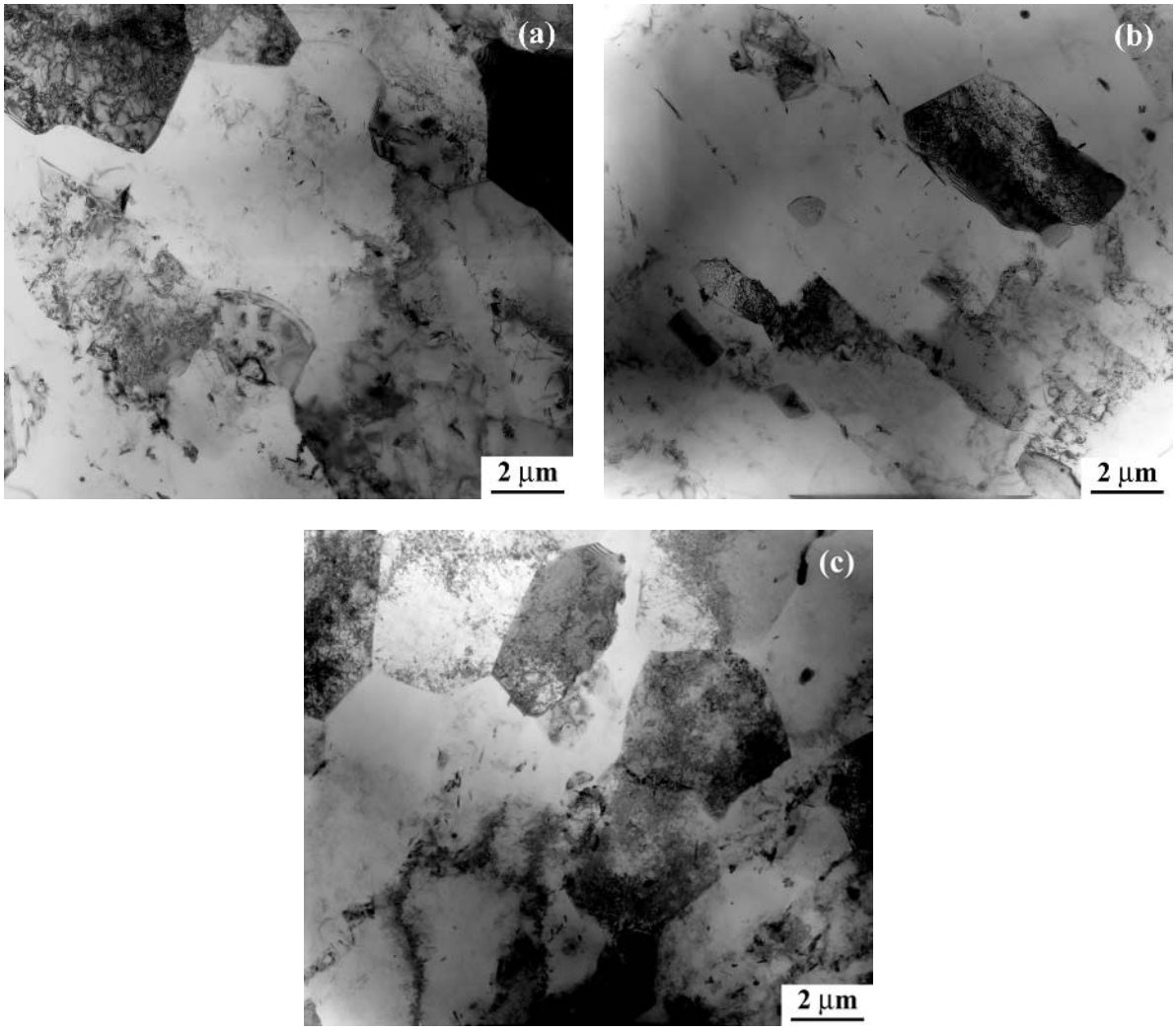

Fig. 9—TEM micrographs showing the microstructure of as-extruded Al-4Mg-1Zr superplastically deformed at 550 °C and an initial strain rate of 1×10^{-2} s^{-1} to a strain of (*a*) and (*b*) 1.0 and (*c*) 1.3.

by high-angle boundaries, were detected (Figure 9(a)). In addition, certain regions still exhibited directionally aligned elongated grains (Figure 9(b)). The microstructure is similar to that in the as-extruded condition. At a strain of 1.3, the majority of grains exhibited an equiaxed shape and consisted of predominantly high-angle boundaries (Figure 9(c)).

The grain size in the deformed specimens is substantially larger than that in the as-extruded sample (Figures 1(a) and 9). No evidence of recrystallization based on nucleation and growth of new grains was detected.

IV. DISCUSSION

A. *Microstructural Characteristics*

1. *As-extruded alloy*

Figure 1 showed that the microstructure of the as-extruded Al-4Mg-1Zr consisted predominantly of low-angle grain boundaries. The generation of such a microstructure is attributed to two factors. First, the presence of the dispersion of fine Al_3Zr particles will hinder recrystallization. Second, the strain produced by the extrusion process was not large enough to induce recrystallization.

Grain-boundary sliding is the primary superplastic deformation mechanism, and the low-angle grain boundaries are generally believed to be not suitable for GBS.[26,27,28] As will be discussed in Section IV–B, fine subgrains converted gradually to high-angle grains with high-temperature deformation, resulting in the observation of HSRS in as-extruded Al-4Mg-1Zr.

2. *The FSP alloy*

Friction stir welding/processing generates significant frictional heating and extensive plastic deformation, thereby creating fine and equiaxed recrystallized grains in the stirred zone.[5,6,8–15] Processing parameters such as tool rotation rate, traverse speed, tool geometry, vertical pressure, and temperature of the workpiece directly affect the material flow pattern and the level of microstructural refinement. In the friction stir welded and FSP aluminum alloys, grain sizes ranging from 0.8 to 12 μm have been reported by various investigators.[5,6,8–15] Recently, the high ratio of the tool's traverse speed/rotation rate was reported to be beneficial to reducing the grain size in the nugget zone.[12,29] For example, increasing the ratio of the tool traverse speed/rotation rate from 4 ipm/400 rpm to 6 ipm/350 rpm reduced the grain size from 7.5 to 3.8 μm in FSP 7075Al.[12] Compared to the processing parameter (6 ipm/350 rpm) for producing a 3.8 μm grain size in FSP 7075Al, a lower ratio of the tool traverse speed/rotation rate (4 ipm/350 rpm) was adopted for the present Al-4Mg-1Zr. However, a much finer grain size of 1.5 μm was generated by friction stir processing in the Al-4Mg-1Zr (Figure 1(b)). This shows that both the friction stir processing parameter and matrix chemistry exert a significant effect on the FSP aluminum alloy microstructure. Growth of recrystallized grains in the nugget zone occurs during the FSW/friction stir processing thermal cycle.[8–11] A recent investigation on FSP 7050Al revealed that the initial size of newly recrystallized grains is on the order of 25 to 100 nm.[30] When heated for 1 to 4 minutes at 350 °C to 450 °C, these grains grow to 2 to 5 μm, a size equivalent to that found in FSP aluminum alloys.[30] For the present Al-4Mg-1Zr, the fine Al_3Zr dispersoids effectively impede the growth of recrystallized grains at high temperature. Thus, the grain size obtained in FSP Al-4Mg-1Zr was much smaller than that in FSP 7075Al.[12]

The measurement of Al_3Zr dispersoids shows that the average size of Al_3Zr dispersoids in FSP Al-4Mg-1Zr is similar to that in the extruded alloy. This indicates that Al_3Zr dispersoids did not coarsen during friction stir processing. This is attributed to the relatively brief duration of the friction stir processing thermal cycle. The FSW/friction stir processing thermal cycle is generally reported to be less than 1 minute, with peak temperatures of 400 °C to 500 °C.[8,9,10] During such a thermal cycle, Al_3Zr dispersoids are stable.

B. *Microstructural Evolution during Superplastic Deformation*

Figure 9 shows that with superplastic straining, the predominantly low-angle grains in the as-extruded condition converted to equiaxed high-angle grains. However, some fraction of low-angle grains remained even after a strain of 1.3. Further, Figure 9 shows the existence of dislocations within grains. A similar microstructural evolution was observed in several as-rolled aluminum alloys having a nonrecrystallized microstructure, such as 7474Al-0.7Zr,[26] Al-6Cu-0.4Zr and Al-0.92Mn-0.3Zr,[31] Al-10Mg-0.1Zr,[32] and Al-6Mg-0.3Sc.[33]

Matsuki *et al.*[26] reported that for as-cold-rolled 7474Al-0.7Zr, the misorientation of sub-boundaries increased with increasing strain at 520 °C and an initial strain rate of 2.5×10^{-1} s^{-1}. After an elongation of 117 pct, the fraction of grain boundaries with a misorientation of <5 deg decreased from 70 to 18 pct, that with a misorientation of 5 to 15 deg increased from 15 to 38 pct, and that with a misorientation of ≥ 15 deg increased from 15 to 45 pct. Such a microstructural transformation has been suggested to be due to a continuous recrystallization process during the initial stage of hot deformation.[26,32–36] This is characterized by the development of moderate misorientations between adjacent subgrains by means of absorption of lattice dislocations into sub-boundaries.[27,33,37] The observation of dislocations within grains in deformed materials has been interpreted as evidence of an accommodation mechanism for GBS involving the generation and motion of dislocations.[26,31,32]

As presented in Section III–C, in the initial stage of superplastic deformation of as-extruded Al-4Mg-1Zr, some grains took part in GBS individually and some by sliding as grain groups; *i.e.,* CGBS was detected (Figure 7(a)). With increasing strain, the fraction of grains sliding as individual grains increased (Figures 7(b) through (d)). This can be explained by the microstructural evolution of the as-extruded alloy with strain. The as-extruded Al-4Mg-1Zr is characterized by predominantly low-angle grain boundaries. Therefore, at the initial stage of superplastic deformation, GBS can occur only for grains with high-angle boundaries, or with intermediate-angle boundaries having a misorientation >5 deg as will discussed in Section IV–D. Furthermore, grain groups in which adjacent grains have a low misorientation slide as a group on boundaries with a high misorientation.[38,39,40] With increasing strain, the low-angle grain boundaries gradually convert to high-angle boundaries. Thus, the fraction of grains involved in individual GBS increases with increasing strain. A low strain rate and high temperature are beneficial for converting low-angle grain boundaries to high-angle grain boundaries. Therefore, with decreasing strain rate or increasing temperature, the fraction of grains involved in GBS increases.

For the FSP alloy, the initial microstructure consisted of predominantly high-angle grain boundaries. Therefore, most

grains took part in GBS, and no CGBS was detected on the surfaces of deformed specimens (Figure 8(b)). However, significant concurrent grain growth occurred during superplastic deformation (Figure 8(b)).

C. *Superplastic Behavior*

1. *As-extruded alloy*

Mishra *et al.*[41] analyzed the superplastic deformation behavior of a number of powder metallurgy (PM)–processed aluminum alloys and composites. They classified the stress-strain curves into four different types. The first was a well-behaved stress-strain curve, where the flow stress remained almost constant during the superplastic flow, and they referred to this as type F (flat). The second was referred to as type H (hardening) and was characterized by continuous strain hardening up to substantial strain values. The third type of stress-strain curve showed continuous strain softening and was referred to as type S (softening). The fourth was referred to as type C (complex), and represented a more complicated stress-strain behavior; *i.e.,* obvious initial strain hardening and significant subsequent softening. For the type-C stress-strain curve, Mishra *et al.* suggested that the initial microstructure consisted of predominantly low-angle boundaries, and these low-angle boundaries changed to high-angle ones with deformation as more lattice dislocations were pumped into the low-angle boundaries. A number of TEM studies dealing with the measurement of boundary misorientation with strain have provided support for this suggestion.[26,31–33]

Figure 2 shows that the stress-strain curves obtained in as-extruded Al-4Mg-1Zr at temperatures <565 °C or initial strain rates of $>3 \times 10^{-2}\ s^{-1}$ were characterized by obvious initial strain hardening and significant subsequent strain softening. These curves are consistent with the type-C curves defined by Mishra *et al.*[41] Therefore, strain softening in as-extruded Al-4Mg-1Zr is believed to be due to the gradual transformation of subgrains to grains with deformation, as evidenced by TEM examination (Figure 9). Such a transformation is generally accompanied by a reduction in flow stress, *i.e.,* strain softening. However, the stress-strain curves obtained in as-extruded Al-4Mg-1Zr at temperatures ≥ 565 °C or initial strain rates of $\leq 3 \times 10^{-2}\ s^{-1}$ consists of three stages, *i.e.,* initial strain hardening, subsequent strain softening, and secondary strain hardening. Clearly, these stress-strain curves are quite different from those summarized by Mishra *et al.* However, if we only consider the stages of initial strain hardening and subsequent strain softening, the stress-strain curves at temperatures ≥ 565 °C or initial strain rates of $\leq 3 \times 10^{-2}\ s^{-1}$ are consistent with the type-C curves.[41] Therefore, strain softening is still likely associated with the gradual transformation of subgrains to grains with deformation. The secondary strain hardening observed at temperatures ≥ 565 °C or initial strain rates of $\leq 3 \times 10^{-2}\ s^{-1}$ are believed to be related to the concurrent grain growth. Higher temperatures and lower strain rates are not only beneficial to the transformation of subgrains to grains, but also promote the concurrent growth of transformed grains, as evidenced by SEM examinations on surfaces of failed specimens. Thus, as-extruded Al-4Mg-1Zr deformed at higher temperatures of ≥ 565 °C or lower initial strain rates of $\leq 3 \times 10^{-2}\ s^{-1}$ exhibited not only higher superplastic ductility, but also secondary strain hardening after the transformation of subgrains to grains was complete.

Due to the fine subgrain size and the transformation of subgrains to grains with deformation, a high superplastic ductility is expected in as-extruded Al-4Mg-1Zr. As shown in Figure 3, a maximum superplastic ductility of 1015 pct was obtained at 580 °C and an initial strain rate of $1 \times 10^{-2}\ s^{-1}$; *i.e.,* HSRS was obtained in as-extruded Al-4Mg-1Zr. In a previous study, Grimes *et al.*[18] reported that simple two-step processing (extrusion plus cold rolling) can result in HSRS in Al-Mg-Zr with strains >500 pct at a strain rate of $1 \times 10^{-2}\ s^{-1}$. However, the temperature range investigated by Grimes *et al.* was 450 °C to 550 °C, and no optimum superplastic deformation temperature was identified in as-cold-rolled Al-4Mg-1Zr. The present study indicates that the optimum superplastic deformation temperature is 580 °C for as-extruded Al-4Mg-1Zr at an initial strain rate of $1 \times 10^{-2}\ s^{-1}$. Above 580 °C, superplasticity was reduced rapidly with increased temperature.

In the past two decades, HSRS has been investigated extensively because of its significant engineering value. This HSRS has been observed in a number of aluminum-based alloys: *i.e.,* composites,[42,43,44], mechanically alloyed (MA) alloys,[45] PM alloys,[46,47] Zr- or Sc-modified alloys, [33,47–50] and fine-grained alloys produced by severe plastic deformation.[50,51,52] However, the origin of HSRS is not well understood. The appearance of a suitable amount of liquid phases[43–45,48,53] or a fine grain size[12,41,54] has been suggested as a possible origin.

To verify if the origin of HSRS in as-extruded Al-4Mg-1Zr is associated with partial melting, DTA was conducted. Partial melting was determined to occur at a temperature of 590.9 °C for as-extruded Al-4Mg-1Zr. This is consistent with the Al-Mg phase diagram.[55] Thus, the optimum superplastic deformation temperature is 10 °C lower than the partial melting temperature. Clearly, the generation of HSRS in as-extruded Al-4Mg-1Zr was not associated with the appearance of a liquid phase, as in some aluminum-matrix composites and aluminum alloys.[43,44,48] Therefore, HSRS in as-extruded Al-4Mg-1Zr must be attributable to the fine subgrains and the gradual transformation of subgrains to grains. The rapid decrease in superplasticity of as-extruded Al-4Mg-1Zr at temperatures >580 °C was attributed to the appearance of a liquid phase.

The present results indicate that a process as simple as one-step extrusion can yield HSRS in Al-4Mg-1Zr. This shows that Al-4Mg-1Zr is an excellent superplastic aluminum alloy. Better superplastic properties can be expected in the FSP alloy with the generation of fine and equiaxed grains during processing.

2. *The FSP alloy*

Different from those of the as-extruded Al-4Mg-1Zr, the stress-strain curves of the FSP alloy exhibited continuous strain hardening.[20] These types of curves are consistent with the type-H (hardening) stress-strain curves defined by Mishra *et al.*[41] As shown in Figure 1(c), the microstructure of FSP Al-4Mg-1Zr consisted of fine and equiaxed recrystallized grains. This microstructure, produced by friction stir processing, is composed predominantly of high-angle boundaries[6] amenable to GBS. Therefore, in the FSP alloy, no strain softening occurs from the transformation of subgrains to grains. The continuous strain hardening with superplastic deformation is generally associated with concurrent grain

growth.[12,41] The concurrent grain growth during the superplastic deformation of FSP Al-4Mg-1Zr has been verified by SEM observations of the surfaces of the deformed specimens (Figure 8(b)).

In a previous study, a FSP 3.8 μm 7075Al exhibited HSRS at an optimum initial strain rate of 1×10^{-2} s^{-1}.[12] For FSP Al-4Mg-1Zr with a grain size of 1.5 μm, a higher optimum strain rate of 1×10^{-1} s^{-1} was observed. This can be attributed to the high fraction of high-angle grain boundaries following friction stir processing. Superplasticity is often characterized using the generalized constitutive equation:[56]

$$\dot{\varepsilon} = A\frac{DG\mathbf{b}}{\mathrm{k}T}\left(\frac{\mathbf{b}}{d}\right)^{p}\left(\frac{\sigma}{G}\right)^{n} \qquad [1]$$

where $\dot{\varepsilon}$ is the strain rate, A is a dimensionless constant, D is the appropriate diffusivity (lattice or grain boundary), G is the shear modulus, **b** is the Burger's vector, k is the Boltzmann constant, T is the absolute temperature, p is the grain-size exponent, d is the grain size, σ is the applied stress, and n is the stress exponent. Equation [1] shows a grain-size dependence, but does not have a term for the type of grain boundary. An additional term, to account for the nature of grain boundaries, is needed to explain the difference between materials processed by different processing routes, as will discussed in Section IV–D.

3. *Comparison between superplastic behavior of the as-extruded and FSP alloys*

It is evident from Figures 3 and 5 that friction stir processing resulted in significantly enhanced superplasticity and a shift to a higher optimum strain rate (from 1×10^{-2} s^{-1} to 1×10^{-1} s^{-1}) and a lower optimum deformation temperature (from 580 °C to 525 °C). Furthermore, friction stir processing resulted in a significant reduction in flow stress for FSP Al-4Mg-1Zr (Figures 4 and 6). The significantly improved superplastic properties in FSP Al-4Mg-1Zr are attributed to the fine and equiaxed grain microstructure and high percentage of high-angle boundaries.[6]

Equation [1] predicts that the grain-size decrease results in an increase in the optimum strain rate and a decrease in both the optimum deformation temperature and flow stress for a given strain rate. The grain size (1.5 μm) in FSP Al-4Mg-1Zr is only slightly smaller than the subgrain size (1.8 μm) in the as-extruded alloy. Therefore, the difference in the superplastic properties of the two alloys is dominated by different grain-boundary characteristics. As discussed earlier, the as-extruded microstructure consisted of predominantly low-angle boundaries, whereas the FSP alloy contained a high fraction of high-angle boundaries. Low-angle boundaries are not amendable to GBS and must be transformed to high-angle boundaries for superplasticity. Therefore, the as-extruded Al-4Mg-1Zr exhibited a higher resistance to superplastic flow at the initial stage of deformation. A higher temperature and lower strain rate are beneficial for such a transformation. Accordingly, a higher optimum temperature of 580 °C and lower optimum strain rate of 1×10^{-2} s^{-1} were observed in as-extruded Al-4Mg-1Zr.

D. *Deformation Mechanism*

Al-Mg alloys are known to exhibit Class I solid behavior, namely, deformation is controlled by solute-drag on gliding dislocations with a stress exponent of 3 (strain-rate sensitivity of ~0.33).[57,58,59] For a fine-grained structure, GBS with a stress exponent of 2 (strain-rate sensitivity of 0.5) is also expected to operate under certain test conditions. Since solute drag and GBS are two independent mechanisms, the deformation in Al-Mg alloys may be controlled simultaneously by both mechanisms or predominantly by one of them. A change of deformation mechanism is also expected with a change in test conditions.

As shown in Figures 4 and 6, the strain-rate sensitivity increases continuously with increasing initial strain rate from 1×10^{-3} s^{-1} to 1 s^{-1} for both the as-extruded and FSP Al-4Mg-1Zr. Similar behavior was also observed in a number of PM aluminum alloys[47,60] and aluminum-matrix composites.[61,62,63] This behavior is different from FSP 7075Al, in which constant strain-rate sensitivities were observed throughout the strain-rate range of 1×10^{-3} s^{-1} to 1×10^{-1} s^{-1}.[12] The trend observed in Al-4Mg-1Zr indicates that either a threshold stress is operative or the deformation mechanism changes. The solute-drag mechanism in Al-Mg alloys usually takes place at intermediate temperatures around 300 °C.[59] For example, in an investigation of the high-temperature deformation behavior of the Al-6Mg-0.3Sc alloy, Nieh *et al.*[33] observed that the rate-controlling deformation mechanism at 350 °C was solute drag–controlled dislocation glide ($m \sim 0.33$), whereas the GBS process prevailed at 475 °C (m value close to 0.5). Because the superplastic data in Figures 4 and 6 were obtained at 425 °C to 580 °C in fine-grained structures, solute drag is unlikely to be the rate-controlling deformation mechanism for the present Al-4Mg-1Zr. Therefore, it is very likely that a threshold stress is operative in both the extruded and FSP Al-4Mg-1Zr.

Mishra *et al.*[41] have analyzed superplasticity data for a number of PM aluminum alloys. They observed a threshold stress–type behavior in aluminum alloys with second-phase particles. Considering the high density of fine Al_3Zr particles dispersed throughout the matrix, the continuous increase in the strain-rate sensitivity with increasing initial strain rate for both as-extruded and FSP Al-4Mg-1Zr is very likely associated with the presence of a threshold stress. In this case, the superplastic deformation behavior of the Al-4Mg-1Zr can be described by a modified relationship for superplasticity in fine-grained aluminum alloys:[41]

$$\dot{\varepsilon} = 40\frac{D_0E\mathbf{b}}{\mathrm{k}T}\exp\left(-\frac{84{,}000}{\mathrm{R}T}\right)\left(\frac{\mathbf{b}}{d}\right)^{2}\left(\frac{\sigma-\sigma_0}{E}\right)^{2} \qquad [2]$$

where D_0 is the pre-exponential constant for grain-boundary diffusivity, E is the Young's modulus, R is the gas constant, and σ_0 is the threshold stress.

The superplastic data of both as-extruded and FSP Al-4Mg-1Zr were examined using the threshold-stress approach. Threshold-stress values at various temperatures were estimated by an extrapolation technique from the plots of $\dot{\varepsilon}^{1/2}$ vs the flow stress on double-linear scales for as-extruded and FSP Al-4Mg-1Zr. The experimentally determined threshold stress decreases with increasing temperature (Table I). Similar observations have been made by other investigators in a number of aluminum alloys and aluminum-matrix composites.[41,64–66]

By introducing a threshold stress, superplastic data from both as-extruded and FSP Al-4Mg-1Zr were plotted in

Table I. Threshold Stress (MPa) Determined Experimentally for As-Extruded and FSP Al-4Mg-1Zr

Materials	425 °C	450 °C	500 °C	525 °C	550 °C	575 °C	580 °C
As-extruded	—	12.36	6.74	5.96	3.91	3.00	1.87
FSP	5.02	3.67	0.81	0.29	—	—	—

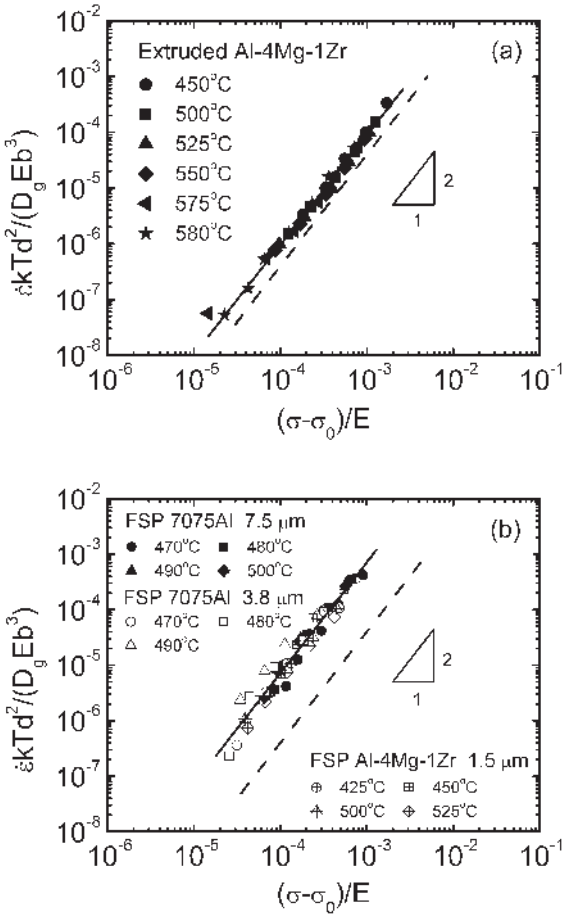

Fig. 10—Variation of $\dot{\varepsilon}\,\mathrm{k}Td^2/D_gE\mathbf{b}^3$ with normalized effective stress, $(\sigma - \sigma_0)/E$, for (*a*) as-extruded Al-4Mg-1Zr and (b) FSP Al-4Mg-1Zr and 7075Al (dashed line represents Eq. [2]).

Figures 10(a) and (b) as $(\dot{\varepsilon}\mathrm{k}Td^2/D_g\,E\mathbf{b}^3)$ vs $(\sigma - \sigma_0)/E$. For comparison, a dashed line predicted by Eq. [2] was also included. Figure 10 reveals three important observations. First, the temperature dependence of superplastic flow for both as-extruded and FSP Al-4Mg-1Zr is similar to the activation energy for aluminum grain-boundary self-diffusion. Second, the data of the two alloys fit straight lines with a slope of 2 after introducing a threshold stress. This illustrates a threshold-type deformation behavior with a stress exponent of 2 ($\dot{\varepsilon} \propto (\sigma - \sigma_0)^2$) for both alloys. Third, while the normalized data of the as-extruded Al-4Mg-1Zr are very close to the prediction by Eq. [2], the FSP Al-4Mg-1Zr exhibited enhanced kinetics. The GBS models of Mukherjee,[67] Arieli and Mukherjee,[68] and Ball and Hutchison[69] predict a stress exponent of 2, an inverse grain-size dependence of 2, and an activation energy close to that for grain-boundary self-diffusion. Thus, Figure 10 show that GBS is the main superplastic deformation mechanism for both extruded and FSP Al-4Mg-1Zr.

Subgrain boundaries are generally considered immobile with respect to grain sliding.[70] However, superplastic investigations of aluminum alloys with a nonrecrystallized starting microstructure suggested that the subgrain boundaries with a misorientation >5 deg play an important role through boundary sliding in the initial stage of superplastic deformation.[26,31,32] Nes[31] interpreted the deformation behavior of Al-6Cu-0.4Zr and Al-0.92Mn-0.3Zr as evidence for GBS in microstructures, where the average boundary misorientation is 5 to 7 deg. Furthermore, Hales and McNelley[32] also suggested that the boundaries in Al-10Mg-0.1Zr behaved as high-angle boundaries, even with a misorientation less than 10 deg at the onset of deformation. Similarly, Matsuki *et al.*[26] pointed out that even the boundary sliding on the sub-boundaries with a 5 to 15 deg misorientation could contribute greatly to deformation. For the present as-extruded Al-4Mg-1Zr with predominant low-angle boundaries, it is believed that the boundaries with a misorientation >5 deg would slide and contribute to deformation in the initial stage of superplastic deformation. The TEM examinations of extruded Al-4Mg-1Zr after deformation provide support for this suggestion. Further, the transformation of low-angle boundaries to high-angle boundaries is a gradual process, because low-angle boundaries could be observed in localized regions even after deformation to a strain of 1.3.

In a previous study,[12] FSP 7075Al exhibited enhanced kinetics compared to the prediction by Eq. [2]. Therefore, it is of interest to check if FSP 7075Al and Al-4Mg-1Zr exhibit similar kinetics. In Figure 10(b), the superplasticity data of two FSP 7075Al specimens with grain sizes of 3.8 and 7.5 μm are plotted. No threshold stress was observed for superplastic deformation of FSP 7075Al. Clearly, superplastic data from three FSP aluminum alloys merge well onto a single line with a slope of 2. The dimensionless constant is determined to be 700. This shows that the superplastic behavior of both FSP Al-4Mg-1Zr and 7075Al can be described by a united constitutive equation:

$$\dot{\varepsilon} = 700\,\frac{D_0E\mathbf{b}}{\mathrm{k}T}\exp\left(-\frac{84{,}000}{\mathrm{R}T}\right)\left(\frac{\mathbf{b}}{d}\right)^2\left(\frac{\sigma-\sigma_0}{E}\right)^2 \quad [3]$$

The dimensionless constant in Eq. [3] is more than one order of magnitude larger than that in Eq. [2] and that (25 to 50) in the GBS models of Mukherjee[67] and Arieli and Mukherjee,[68] exhibiting similar enhancement in kinetics in both FSP aluminum alloys. Considering that FSP Al-4Mg-1Zr and 7075Al have different chemistries and grain sizes and exhibited different superplastic deformation behaviors (there is a threshold stress for FSP Al-4Mg-1Zr, but not for FSP 7075Al), Eq. [3] implies that enhanced kinetics may be a common feature for FSP aluminum alloys. Clearly, conventional GBS models are not able to predict the deformation kinetics in FSP aluminum alloys, although the parametric dependencies are consistent.

As pointed out previously, the microstructure of FSP aluminum alloys is characterized by fine and high-angled grains. The fraction of high-angle boundaries is as high as 85 to

95 pct.[6,71] This ratio is significantly higher than that obtained in conventional TMP aluminum alloys, with a typical ratio of 50 to 65 pct.[16,72] A high percentage of high-angle boundaries makes the contribution of GBS to strain significantly higher, thereby resulting in enhanced kinetics. It is proposed that the dimensionless constant in Eq. [3] is a function of the fraction of high-angle boundaries and increases as the fraction of high-angle boundaries increases. The suitability of Eq. [3] for FSP aluminum alloys is under further investigation. Furthermore, an attempt is being made to correlate the dimensionless constant in Eq. [3] with the fraction of high-angle boundaries to establish a better constitutive relationship for superplastic deformation of fine-grained aluminum alloys.

V. CONCLUSIONS

1. The microstructure of as-extruded Al-4Mg-1Zr consisted predominantly of low-angle grains aligned along the extrusion direction. Friction stir processing converted the low-angle grain boundaries to high-angle grain boundaries and led to fine and equiaxed grains.
2. The stress-strain curves for extruded Al-4Mg-1Zr exhibited distinct strain softening after initial strain hardening due to conversion of low-angle grain boundaries to high-angle ones. However, the FSP alloy exhibited predominant strain hardening due to concurrent grain growth.
3. As-extruded Al-4Mg-1Zr exhibited HSRS. A maximum ductility of 1015 pct was obtained at 580 °C and an initial strain rate of 1×10^{-2} s^{-1}.
4. Friction stir processing resulted in considerably enhanced superplasticity, significantly reduced flow stress, and a shift to a higher optimum strain rate and lower optimum temperature. A maximum superplastic ductility of 1280 pct was observed at 525 °C and an initial strain rate of 1×10^{-1} s^{-1}.
5. The strain-rate sensitivity of both as-extruded and FSP Al-4Mg-1Zr increased continuously with increasing strain rate from 1×10^{-3} s^{-1} to 1 s^{-1}, indicating the presence of a threshold stress for superplastic deformation.
6. The SEM examinations of the surfaces of deformed specimens revealed distinct evidence of GBS. For the as-extruded alloy, grains involved in GBS increased with strain. In addition, CGBS was observed, in particular in the initial stage of superplastic deformation. For the FSP alloy, no CGBS was detected.
7. An analysis of the superplastic data of as-extruded and FSP Al-4Mg-1Zr revealed a stress exponent of 2 and an activation energy close to that for grain-boundary self-diffusion. This indicates that GBS is the main superplastic deformation mechanism for both as-extruded and FSP Al-4Mg-1Zr.
8. While the superplastic data of as-extruded Al-4Mg-1Zr exhibited kinetics similar to that in fine-grained aluminum alloys, FSP Al-4Mg-1Zr exhibited significantly enhanced kinetics, which is attributed to the higher fraction of high-angle grain boundaries in FSP aluminum alloys.

ACKNOWLEDGMENTS

The authors gratefully acknowledge the support of the National Science Foundation through Grant No. DMR-0076433 and the Missouri Research Board for the acquisition of a friction stir welding and processing machine; the National Science Foundation through Grant Nos. DMI-0085044 and DMI-0323725, Dr. Jian Cao, Program Manager; and the Office of Naval Research through Grant No. N00014-00-C-0520, Drs. Leo Christodoulou (DARPA) and Julie Christodoulou (ONR), Program Managers.

REFERENCES

1. N.E. Paton, C.H. Hamilton, J. Wert, and M. Mahoney: *J. Met.,* 1982, vol. 34, pp. 21-27.
2. J. Xinggang, C. Jiangzhong, and M. Longxiang: *Acta Metall. Mater.,* 1993, vol. 41, pp. 2721-27.
3. V.M. Segal: *Mater. Sci. Eng. A,* 1995, vol. A197, pp. 157-64.
4. R.Z. Valiev: *Mater. Sci. Eng. A,* 1993, vol. A168, pp. 141-48.
5. R.S. Mishra, M.W. Mahoney, S.X. McFadden, N.A. Mara, and A.K. Mukherjee: *Scripta Mater.,* 2000, vol. 42, pp. 163-68.
6. R.S. Mishra and M.W. Mahoney: *Mater. Sci. Forum,* 2001, vols. 357–359, pp. 507-12.
7. W.M. Thomas, E.D. Nicholas, J.C. Needham, M.G. Murch, P. Templesmith, and C.J. Dawes: G.B. Patent Application No. 9125978.8, Dec. 1991.
8. S. Benavides, Y. Li, L.E. Murr, D. Brown, and J.C. McClure: *Scripta Mater.,* 1999, vol. 41, pp. 809-15.
9. M.W. Mahoney, C.G. Rhodes, J.G. Flintoff, R.A. Spurling, and W.H. Bingel: *Metall. Mater. Trans. A,* 1998, vol. 29A, pp. 1955-64.
10. C.G. Rhodes, M.W. Mahoney, W.H. Bingel, R.A. Spurling, and C.C. Bampton: *Scripta Mater.,* 1997, vol. 36, pp. 69-75.
11. K.V. Jata and S.L. Semiatin: *Scripta Mater.,* 2000, vol. 43, pp. 743-49.
12. Z.Y. Ma, R.S. Mishra, and M.W. Mahoney: *Acta Mater.,* 2002, vol. 50, pp. 4419-30.
13. Z.Y. Ma and R.S. Mishra: *Acta Mater.,* 2003, vol. 51, pp. 3551-69.
14. I. Charit, R.S. Mishra, and M.W. Mahoney: *Scripta Mater.,* 2002, vol. 47, pp. 631-36.
15. M. Mahoney, R.S. Mishra, T. Nelson, J. Flintoff, R. Islamgaliev, and Y. Hovansky: in *Friction Stir Welding and Processing,* K.V. Jata, M.W. Mahoney, R.S. Mishra, and D.P. Field, eds., TMS, Warrendale, PA, 2001, pp. 183-94.
16. T.R. McNelley and M.E. McMahon: *Metall. Mater. Trans. A,* 1997, vol. 28A, pp. 1879-87.
17. N. Ridley, E, Cullen, and F.J. Humphreys: in *Superplasticity and Superplastic Forming,* A.K. Ghosh and T.R. Bieler, eds., TMS, Warrendale, PA, 1998. pp. 65-74.
18. R. Grimes, R.J. Dashwood, A.W. Harrison, and H.M. Flower: *Mater. Sci. Technol.,* 2000, vol. 16, pp. 1334-39.
19. R.J. Dashwood, R. Grimes, A.W. Harrison, and H.M. Flower: *Mater. Sci. Forum,* 2001, vols. 357–359, pp. 339-44.
20. Z.Y. Ma, R.S. Mishra, M.W. Mahoney, and G. Grimes: *Mater. Sci. Eng. A,* 2003, vol. A351, pp. 148-53.
21. T.R. Chen and J.C. Huang: *Metall. Mater. Trans. A,* 1999, vol. 30A, pp. 53-64.
22. M.T. Perez-Prado, G. Gonzalez-Doncel, O.A. Ruano, and T.R. McNelley: *Acta Mater.,* 2001, vol. 49, pp. 2259-68.
23. Y.N. Wang and J.C. Huang: *Scripta Mater.,* 2003, vol. 48, pp. 1117-22.
24. M.G. Zelin and A.K. Mukherjee: *Acta Metall. Mater.,* 1995, vol. 43, pp. 2359-72.
25. M.G. Zelin: *J. Mater. Sci. Lett.,* 1996, vol. 15, pp. 2068-70.
26. K. Matsuki, T. Iwaki, M. Tokizawa, and Y. Murakami: *Mater. Sci. Technol.,* 1991, vol. 7, pp. 513-19.
27. T. Watanabe: *Metall. Trans. A,* 1983, vol. 14A, pp. 531-45.
28. T. Watanabe, M. Yamada, S. Shima, and S. Karashima: *Phil. Mag.,* 1979, vol. 40, pp. 667-83.
29. H. Salem, A. Reynolds, and J. Lyons: *Lightweight Alloys for Aerospace Applications,* K. Jata, E.W. Lee, W. Frazier, and N.J. Kim, eds., TMS, Warrendale, PA, 2001, pp. 141-50.
30. C.G. Rhodes, M.W. Mahoney, W.H. Bingel, and M. Calabrese: *Scripta Mater.,* 2003, vol. 48, pp. 1451-55.
31. E. Nes: in *Superplasticity,* B. Baudelet and M. Suéry, eds., CNRS, Grenoble, France, 1985, ch. 7.
32. S.J. Hales and T.R. McNelley: *Acta Mater.,* 1988, vol. 36, pp. 1229-39.
33. T.G. Nieh, R. Kaibyshev, L.M. Hsiung, N. Nguyen, and J. Wadsworth: *Scripta Mater.,* 1997, vol. 36, pp. 1011-16.
34. E. Nes: *J. Mater. Sci.,* 1978, vol. 13, pp. 2052-55.

35. E. Nes: *Met. Sci.,* 1979, vol. 13, pp. 211-15.
36. R.H. Bricknell and J.W. Edington: *Metall. Trans. A,* 1979, vol. 10A, pp. 1257-63.
37. H. Kokawa, T. Watanabe, and S. Karashima: *Scripta Metall.,* 1983, vol. 17, pp. 1155-59.
38. V.V. Astanin, O.A. Kaibyshev, and S.N. Faizova: *Scripta Metall.,* 1991, vol. 25, pp. 2663-68.
39. M.G. Zelin, T.R. Bieler, and A.K. Mukherjee: *Metall. Trans. A,* 1993, vol. 24A, pp. 1208-12.
40. M.G. Zelin, R.W. James, and A.K. Mukherjee: *J. Mater. Sci. Lett.,* 1993, vol. 12, pp. 176-78.
41. R.S. Mishra, T.R. Bieler, and A.K. Mukherjee: *Acta Mater.,* 1995, vol. 43, pp. 877-91.
42. L. Geng, T. Imai, J.F. Mao, M. Takagi, and C.K. Yao: *Mater. Sci. Technol.,* 2001, vol. 17, pp. 187-94.
43. M. Mabuchi and K. Higashi: *Phil. Mag. Lett.,* 1994, vol. 70, pp. 1-6.
44. M. Mabuchi and K. Higashi: *Acta Mater.,* 1999, vol. 47, pp. 1915-22.
45. T.G. Nieh, P.S. Gilman, and J. Wadsworth: *Scripta Metall.,* 1985, vol. 19, pp. 1375-78.
46. W.J. Kim and S.H. Hong: *J. Mater. Sci.,* 2000, vol. 35, pp. 2779-84.
47. W.J. Kim, K. Higashi, and J.K. Kim: *Mater. Sci. Eng. A,* 1999, vol. A260, pp. 170-77.
48. R. Kaibyshev, F. Musin, D. Gromov, T.G. Nieh, and D.R. Lesuer: *Scripta Mater.,* 2002, vol. 47, pp. 569-75.
49. T.G. Nieh, L.M. Hsiung, J. Wadsworth, and R. Kaibyshev: *Acta Mater.,* 1998, vol. 46, pp. 2789-2800.
50. K.T. Park, D.Y. Hwang, Y.K. Lee, Y.K. Kim, and D.H. Shin: *Mater. Sci. Eng. A,* 2003, vol. A341, pp. 273-81.
51. S. Lee, M. Furukawa, Z. Horita, and T.G. Langdon: *Mater. Sci. Eng. A,* 2003, vol. A342, pp. 294-301.
52. R.S. Mishra, R.Z. Valiev, S.X. McFadden, R.K. Islamgaliev, and A.K. Mukherjee: *Phil. Mag. A,* 2001, vol. 81, pp. 37-48.
53. A.K. Mukherjee, R.S. Mishra, and T.R. Bieler: *Mater. Sci. Forum,* 1997, vols. 233–234, pp. 217-34.
54. J. Koike, K. Mabuchi, and K. Higashi: *Acta Metall. Mater.,* 1995, vol. 43, pp. 199-206.
55. *Smithells Metals Reference Book,* 7th ed., E.A. Brandes and G.B. Brook, eds., Butterworth–Heinemann., Oxford, United Kingdom, 1997, p. 41.
56. A.K. Mukherjee, J.E. Bird, and J.E. Dorn: *Trans. ASM,* 1969, vol. 62, pp. 155-79.
57. O.D. Sherby and P.M. Burke: *Progr. Mater. Sci.,* 1967, vol. 13, pp. 325-90.
58. K.L. Murty, F.A. Mohamed, and J.E. Dorn: *Acta Metall.,* 1972, vol. 20, pp. 1009-18.
59. H. Oikawa, K. Sugawara, and S. Karashima: *Trans. JIM,* 1978, vol. 19, pp. 611-16.
60. T.G. Nieh and J. Wadsworth: *Mater. Sci. Forum,* 1997, vols. 243–245, pp. 257-66.
61. H. Iwasaki, T. Mori, M. Mabuchi, and K. Higashi: *Metall. Mater. Trans. A,* 1998, vol. 29A, pp. 677-83.
62. G.Q. Tong and K.C. Chan: *Mater. Sci. Eng. A,* 2000, vol. A286, pp. 218-24.
63. W.J. Kim and O.D. Sherby: *Acta Mater.,* 2000, vol. 48, pp. 1763-74.
64. Y. Li and TG. Langdon: *Acta Mater.,* 1999, vol. 47, pp. 3395-3403.
65. F.U. Enikeev: *Mater. Sci. Eng. A,* 2000, vol. A276, pp. 22-31.
66. W.J. Kim, J.H. Yeon, D.H. Shin, and S.H. Hong: *Mater. Sci. Eng. A,* 1999, vol. A269, pp. 142-51.
67. A.K. Mukherjee: in *Grain Boundaries in Engineering Materials,* J.L. Walter *et al.,* eds., Claiton Publishing, Baton Rouge, LA, 1975, p. 93.
68. A. Arieli and A.K. Mukherjee: *Mater. Sci. Eng.,* 1980, vol. 45, pp. 61-70.
69. A. Ball and M.M. Hutchison: *Met. Sci. J.,* 1969, vol. 3, pp. 1-7.
70. H. Kokawa, T. Watanabe, and S. Karashima: *Phil. Mag. A,* 1981, vol. 44, pp. 1239-54.
71. A.F. Norman, I. Brough, and P.B. Prangnell: *Mater. Sci. Forum,* 2000, vols. 331–337, pp. 1713-18.
72. M. Eddahbi, T.R. McNelley, and OA. Ruano: *Metall. Mater. Trans. A,* 2001, vol. 32A, pp. 1093-1102.